East European Journal of Physics. 1. 378-387 (2026)
DOI:10.26565/2312-4334-2026-1-45 ISSN 2312-4334

TOPOLOGICAL FEATURES OF CONDUCTIVE NETWORK FORMATION IN METAL–POLYMER COMPOSITES WITH VARYING FILLER PARTICLE SIZES

Zafarjon M. Khusanov[1]*, Fakhriddin T. Boymuratov[2], Sardor G'. To'ychiyev[1]
[1]*Cyber University, Nurafshan, Uzbekistan*
[2]*Alfraganus University, Tashkent, Uzbekistan*
**Corresponding Author e-mail: zafarjonxusanov62@gmail.com*
Received December 10, 2025; revised February 9, 2026; accepted February 13, 2026

The topology of the infinite cluster in polymer composites containing micro- and nanoparticles of Ni was investigated, enabling a quantitative evaluation of how the size of conducting particles influences the percolation transition and the structure of the conductive network. The use of nanosized Ni reduces the critical concentration to Vs ≈ 0.105, compared with Vs ≈ 0.21 for microparticles, increases the parameter σ_1 by more than an order of magnitude, and results in a sharper, more localized percolation transition. The cluster structure exhibits pronounced fractal–hierarchical features: the fractal dimension of the backbone is 1.6-1.8 and that of the dangling ends is 1.9-2.1. The cluster density, correlation radius, and topological parameters follow power-law relations typical of three-dimensional percolation ($\nu = 0.85$). At high concentrations of the conducting phase ($V \geq 0.3$), the asymptotic conductivity reaches 63 $\Omega^{-1}\cdot cm^{-1}$ in nanocomposites versus 8 $\Omega^{-1}\cdot cm^{-1}$for microparticle-based materials. These findings confirm the high efficiency of Ni nanoparticles in forming an extended, interconnected, and branched conductive network, providing the foundation for next-generation high-conductivity composites.
Keywords: *Polymer composites; Nickel nanoparticles; Microparticles; Infinite cluster; Conducting network; Asymptotic conductivity; Topological parameters; Three-dimensional percolation*
PACS: 78.30.Am

INTRODUCTION

As is well known, metal–polymer composites (MPCs) are a class of functional materials in which the metallic phase is dispersed within a polymer matrix, forming a conductive network that combines high electrical conductivity with the flexibility, chemical stability, and manufacturability of polymers. Such materials are widely used in electronics, sensing systems, electromagnetic shielding coatings, antennas, flexible printed circuits, and thermal management systems [1–5]. Their properties are primarily controlled by altering the nature and volume fraction of the metallic filler, as well as the shape, distribution, and size of its particles. These microstructural parameters govern the metallic phase's ability to form a three-dimensional conductive network, or the so-called “infinite cluster,” once a critical concentration—the percolation threshold—is reached [6,7].

The theory of percolation and fractal geometry forms the basis for understanding the mechanisms governing the formation of conductive pathways in heterogeneous systems [8]. According to this theory, as the concentration of the filler increases within the dielectric matrix, the system undergoes a transition from isolated particle clusters to an interconnected network that enables macroscopic conductivity. The morphology and topology of this network are determined by the size, shape, and spatial distribution of the particles, as well as by the nature of their interfacial interactions [9]. The topology of the infinite cluster is characterized by several parameters – such as fractal dimension, coordination number, degree of branching, and contact density – that significantly influence the electrical, thermal, and mechanical properties of the composite [10].

Recent studies confirm that the particle size of the metallic filler is a key factor governing the percolation behavior of MPCs. In particular, the review in [11–13] demonstrated that, at a fixed volume fraction of the filler, an increase in particle dispersity (size distribution width) leads to a higher percolation threshold.

As noted in [14], two nanocomposites containing metallic particles exhibit a high percolation threshold—exceeding 55 vol. %—when the particle size is non-optimal, which is consistent with experimental observations. The use of copper particles coated with silver in a PPS polymer matrix reduces the percolation threshold and increases the effective dielectric permittivity of the composite compared with composites based on pure Cu particles. This improvement is attributed to a more uniform particle distribution and enhanced adhesion to the matrix [15]. Similar trends have been reported for EVA-based composites containing Zn particles, where the relationship between the electrical percolation threshold and mechanical properties is governed by the morphology of the infinite cluster [16]. It has been established that reducing Zn particle size promotes the formation of a more cohesive conductive network, leading to a lower percolation threshold and enhanced electrical conductivity while maintaining mechanical strength.

Numerical models and stochastic finite-element simulations also confirm the decisive role of microstructure in the formation of the cluster network. In polymer composites with magnetic fillers (Fe, Ni), a reduction in particle size results in a pronounced reorganization of the cluster structure: the connectivity density increases, while the average chain length

Cite as: Z.M. Khusanov, F.T. Boymuratov, S.G'. To'ychiyev, East Eur. J. Phys. 1, 378 (2026), https://doi.org/10.26565/2312-4334-2026-1-45

decreases, which affects both the mechanical and magnetic properties of the material [17]. According to the findings in [18], the shape and spatial distribution of particles exert a significant influence on the percolation threshold and dielectric permittivity; moreover, a reduction in filler polydispersity promotes the formation of a more regular fractal cluster structure.

Several recent publications [19–21] highlight the importance of the spatial organization of metallic particles within the matrix and the potential to predict it using modeling approaches. According to the results reported in [15,22], the development of a unified model of electrical and thermal conductivity for composites containing metallic particles of various sizes has shown that reducing the mean particle diameter of Cu and Ag by approximately 20–30% leads to a decrease in the percolation threshold (from ≈4 vol% for pure Cu to ≈ 3 vol% for Ag-coated Cu particles), owing to the increased probability of forming contact bridges. It has also been noted that targeted manipulation of the conductive network topology can be achieved by controlling the spatial distribution of fillers within the polymer matrix, including the combined use of micro- and nanoparticles that form a multilevel conductive structure [23].

Of particular interest are studies linking cluster geometry to the mechanical and dielectric properties of MPCs. The work in [24] demonstrated that rubber-based composites containing metallic magnetic particles exhibit a double percolation threshold, associated with the formation of two distinct types of clusters—local and system-spanning. Similar findings were reported in [25], where polyurethane composites with AlN and BN microparticles were investigated. The authors showed that the network topology near the percolation threshold dictates not only the electrical but also the thermoelectric properties of the material. These observations confirm that variations in particle size and the degree of agglomeration directly influence the morphology of the infinite cluster and, consequently, the overall properties of the composite.

An analysis of the literature indicates that the particle size of the metallic filler plays a decisive role in the formation of the conductive structure in metal–polymer composites. However, most published studies focus either on empirically determining the percolation threshold or on examining the material's macroscopic properties, without a detailed investigation of the cluster network's topology. Insufficient attention has been given to the quantitative characterization of how particle size and its distribution affect the fractal characteristics of the infinite cluster, such as connectivity density, degree of branching, and geometric coherence.

The present study aims to investigate the relationship between the particle size of the metallic filler and the topology of the infinite cluster in metal–polymer composites containing micro- and nanoparticles of nickel (Ni). By combining experimental structural analysis with elements of percolation modeling, the work seeks to elucidate the fundamental patterns governing the evolution of the conductive network morphology as a function of particle size and spatial distribution.

EXPERIMENTAL SAMPLES AND RESEARCH METHODOLOGY

To investigate the effect of metallic particle size on the morphology and conductive properties of the composites, a nanocomposite containing Ni particles was synthesized via thermal decomposition of nickel formate within a polymer matrix. The nanocomposite was prepared via thermal decomposition, analogous to the synthesis of nanoparticles in polyethylene and polypropylene matrices [26,27]. Specifically, nickel formate powder was added to a solution of phenylon in dimethylformamide (4 g of phenylon per 100 g of solvent). After thorough mixing, the mixture was heated to ensure complete removal of the solvent. To prevent aggregation of nickel formate particles, the reaction mixture was ultrasonically processed using a UZDN-1 disperser (22 kHz, 0.3 W). Following solvent evaporation, the resulting material was placed under vacuum and held at 373 K for 1 hour to remove residual solvent. The temperature was then increased to 573 K and maintained for 5 hours, enabling the formation of metallic nanoparticles through the thermal decomposition of nickel formate.

The particle size and spatial distribution within the composites were determined using small-angle X-ray scattering (SAXS), which enables the characterization of inhomogeneities with characteristic dimensions ranging from 5-10 Å to approximately ~10^4 Å [28]. Calculations of the metal particle radius indicated that the nanoparticles did not exceed 30 nm in diameter, consistent with the experimental data.

The microcomposite containing metallic particles was produced by mechanically mixing the metallic powder with the polymer matrix in a planetary mill for 7 hours. The metallic powder itself was obtained by thermally decomposing nickel formate under vacuum at 573 K for 3 hours. The resulting particle diameter ranged from 1 to 3 μm, which was confirmed by transmission electron microscopy (TEM) using a BS242E (Tesla) microscope.

In both types of composites, the metal concentration (V_1) was calculated based on the metallic content of the precursor compound. For electrical measurements, the powder samples were pressed into 15 mm diameter, 2 mm thick pellets using hot pressing. The resistance of the resulting samples was measured according to the procedure described in [29].

RESULTS AND DISCUSSION

In the present study, the topology of the infinite cluster (IC) in polymer matrices containing micro- and nanoparticles of Ni was investigated using percolation theory methods. For these systems, the key characteristics of the IC were determined, including its density, volume fraction, tortuosity, skeletal volume fraction, and number of dead ends, as functions of the metallic particle size.

According to percolation theory [30], the conductivity σ of composites with randomly distributed metallic particles is described by the following relations:

$$\sigma(V_1) = \sigma_1 (V_1 - V_c)^t,\ V_1 > V_s, \tag{1}$$

$$\sigma(V_1) = \sigma_2 (V_c - V_1)^{-q},\ V_1 < V_s, \tag{2}$$

where σ_1 and σ_2 are the conductivities of the metallic particles and the dielectric matrix, respectively; V_1 is the volume fraction of the metallic filler; V_c is the critical concentration at which an infinite cluster is formed; and t and q are the critical exponents, which for three-dimensional systems take values of approximately 1.6–1.8 and 1, respectively.

Percolation theory provides tools for quantitatively describing the topology of the resistance network, in particular the density of the infinite cluster $P(V_1)$, which represents the fraction of sites belonging to the infinite cluster:

$$P(V_1) = V_1' / V_1, \tag{3}$$

where V_1' is the volume fraction of the infinite cluster. For $V_1 < V_s$ *one has* $P(V_1) = 0$, while with increasing V_1 the value of $P(V_1)$ approaches unity. Near the percolation threshold, the density of the infinite cluster follows a power-law dependence [31]

$$P(V_1) = D(V_1 - V_s)^{\beta}, \tag{4}$$

where $D \approx 1$ and β is the critical exponent (for three-dimensional systems $\beta \approx 0.4$).

The length of the backbone of the infinite cluster is evaluated using the model proposed by B. I. Shklovskii [31], in which the IC network is represented as a large, planar fishing net (Fig. 1).

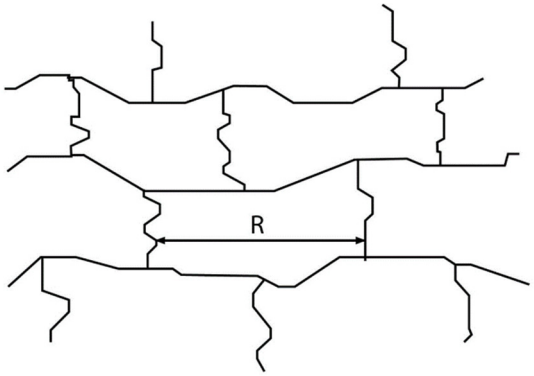

Figure 1. Topology of the Infinite Cluster Backbone

A typical topology of the infinite cluster (IC) backbone in three-dimensional composite systems with conducting particles is shown in Fig. 1. This model is traditionally considered within the framework of percolation theory [32]. The backbone is represented as a network of interconnected conductive paths linked by nodes. The diagram illustrates the primary load-bearing chains that provide a continuous path across the sample and determine the electrical conductivity of the system for $V_1 > V_s$; near the percolation threshold $V_1 \approx V_s$ dead ends account for as much as 80–95% of the IC. A key parameter highlighted in the figure is the correlation radius R (ranging from 10^{-6} to 10^{-3} m for Ni-based composites), which characterizes the characteristic linear dimension of the network cells. Near the percolation threshold, it follows a power-law dependence:

$$R \sim (V_1 - V_s)^{-\nu},\ R = l / \nu \tag{5}$$

where $\nu = 0.85 \pm 0.05$ is the critical exponent of the correlation radius for three-dimensional systems, and l is the lattice period. Also shown are the tortuous (fractal) conductive trajectories arising from the irregular spatial distribution of particles. The tortuosity defines the coefficient ξ, which together with the correlation exponent ν\nuν determines the critical conductivity exponent:

$$t = \xi + \nu, \tag{6}$$

where, for real composites, t typically lies in the range $1.7 \leq t \leq 2.3$, with $\xi \approx 1.2$-1.4

As shown in Fig. 1, the backbone of the infinite cluster represents a fractal network of conductive channels through which the current flows along the longest and most well-connected trajectories. The higher the dispersity of the particles (nanoparticles → greater tortuosity), the larger the contribution of path length to the critical exponent ttt, which reduces the efficiency of the conductive network when the filler content only slightly exceeds the percolation threshold [33].

Based on the proposed model, it has been established that when the wire elements forming the BC skeleton exhibit curvature (Fig. 2, while the distance between their intersection points remains equal to R), the critical exponent of electrical conductivity t exceeds 1.7.

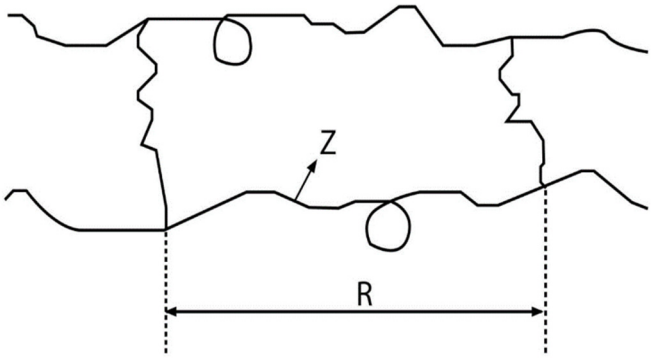

Figure 2. Topology of the Infinite Cluster Skeleton with Curved (Tortuous) Elements

In Figure 2, a representative topological model of the infinite-cluster skeleton formed in composite systems near the percolation threshold is presented. The cluster geometry consists of a sequence of tortuous conducting branches with local widenings and narrow constrictions, which together form the primary framework of the transport network. The characteristic correlation scale R defines the average distance between structurally stable nodes that participate in transmitting flux or electrical current, whereas the quantity Z denotes the direction of the local gradient propagating along a skeleton branch. The critical conductivity exponent t is determined by Eq. (6) as the sum of the index ξ, which accounts for the tortuosity of the conducting filaments, and the correlation-radius index ν. The length of a filament between two intersection points, Z (Fig. 2), is expressed via ξ as

$$Z = l / (V_1 - V_s)^{\xi}, \tag{7}$$

and the ratio of Z to R,

$$\frac{Z}{R} = (V_1 - V_s)^{(\nu-\xi)}, \tag{8}$$

characterizes how many times the skeleton length exceeds R due to the tortuosity of its branches.

The skeleton structure exhibits fractal properties, which is reflected in the values of the fractal dimension $D_f \approx 2.4$-2.6 for three-dimensional systems and in the increased tortuosity of the transport trajectories ($\tau \approx 1.5$-4). The presence of local broadenings and nonuniformly distributed nodes leads to variations in the local connectivity density within the cluster, which in turn affects the effective transport parameters, including electrical conductivity, diffusion, and heat transfer. Such a configuration is characteristic of systems operating in the regime of critical percolation and determines the key features of the macroscopic behavior of the material.

The infinite cluster consists of the backbone and dangling ends [31]. A point is considered to belong to the backbone of the infinite cluster (Fig. 3) if at least two independent paths originate from it, allowing one to reach an infinite distance (point C).

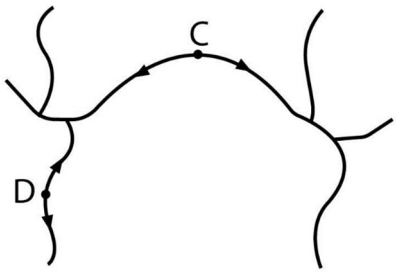

Figure 3. Fragment of the backbone of the infinite cluster with dangling ends.

The fragment of the infinite-cluster backbone shown in Fig. 3 illustrates a typical topology of the conducting network near and above the percolation threshold. The main current-carrying path is formed by the backbone portion of the cluster—a continuous chain of interconnected conducting elements that ensures the macroscopic connectivity of the system. Numerous branch-like "dangling ends" are attached to the backbone; although they do not participate in current transport, they significantly affect the fractal and topological parameters of the infinite cluster. The backbone is characterized by a linear size on the order of $R \sim 10^2$-10^3 nm, which corresponds to the scale of the correlation length ξ near the percolation threshold $V_1 \gtrsim V_s$. The dangling ends have characteristic sizes z ~ 10-100 nm, and their volume fraction in the immediate vicinity of the conduction threshold substantially exceeds that of the backbone bonds, which is consistent with the percolation relations $V_1^{sk} \ll V_1^{m.k}$ [34].

The fractal morphology of the backbone segment of the infinite cluster is directly reflected in the values of the critical exponents that govern the conductivity behavior near the percolation threshold. For three-dimensional composite systems, the following parameters are typical: the critical conductivity exponent lies in the range t = 1.7-2.3, which is consistent with the universal values for three-dimensional percolation systems. The fractal dimension of the current-carrying backbone is $d_{sk} \approx$ 1.6-1.8, whereas the fractal dimension of the branches that do not contribute to charge transport ("dangling ends") is somewhat higher and lies in the range $d_{mk} \approx$ 1.9-2.1. These values confirm that, near the percolation threshold, the structure of the infinite cluster is strongly heterogeneous: the conducting backbone exhibits pronounced tortuosity and reduced dimensionality, while the dangling ends form a more highly branched and spatially dense portion of the cluster [35]. Such a topology determines the characteristic current-flow pathways in percolating composites and strongly influences the magnitude of the macroscopic conductivity.

If only a single path extends from a given point to an infinite distance (for example, point D), that point is regarded as belonging to a dangling end. The total value $P(V_1)$ accounts for all nodes of the infinite cluster, including both backbone nodes and dangling ends. The backbone density $P_{bb}(V_1)$, characterizes the fraction of nodes that belong specifically to the backbone and is defined as

$$P_{sk}(V_1) = V_1^{//} / V_1^{/}, \tag{9}$$

where $V_1^{//}$ is the volume fraction of the backbone of the infinite cluster. According to percolation theory, the ratio $P_{bb}(V_1)/P(V_1)$ can be expressed as

$$\frac{P_{sk}(V_1)}{P(V_1)} = D(V_1 - V_s)^{(2\nu-\beta)}, \tag{10}$$

where D is a numerical coefficient of order unity.

Figure 4 presents a comparison of the experimental data with the theoretical conductivity dependences $\sigma(V)$ for ceramic composites containing nanodispersed (curve 1) and microdispersed (curve 2) nickel.

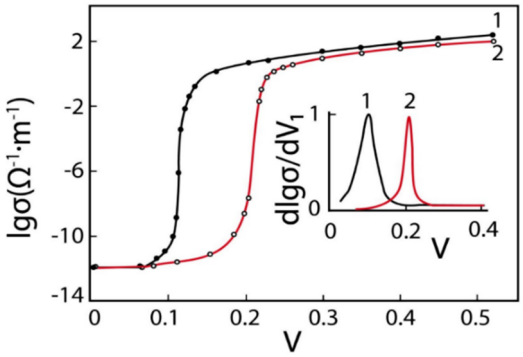

Figure 4. Experimental and theoretical dependencies of electrical conductivity σ on the volume fraction of Ni for composites containing micro- and nanoparticles

Both dependencies exhibit a characteristic percolation transition, accompanied by an abrupt increase in σ by several orders of magnitude upon reaching the critical volume fraction of the conductive filler. Figure 4 also presents the theoretical $\sigma(V_1)$, curves calculated according to expressions (1) and (2). When applying the boundary conditions $V_1 = 0$ and $V_1 = 1$ these relations reduce to the following form [36,37]:

$$\sigma(V_1) = \sigma_1 \left(\frac{V_1 - V_s}{1 - V_s}\right)^t, \; V_1 > V_s, \tag{11}$$

$$\sigma(V_1) = \sigma_2 \left(\frac{V_s - V_1}{V_s}\right)^{-q}, \; V_1 < V_s, \tag{12}$$

where σ_1 and σ_2 are the conductivities of the metallic particles and the dielectric matrix, respectively, V_1 is the volume fraction of the metallic filler, Vc is the percolation threshold, and t and q are the critical exponents characteristic of three-dimensional percolation systems.

The critical volume fraction Vc of Ni particles for the studied composites were determined by differentiating the dependence of lg σ with respect to V_1 (see the inset in Fig. 4). The critical exponent t was evaluated by representing the experimental data in the coordinates

$$lg\sigma = f(lg[(V_1 - V_s)/(1 - V_s)]), \tag{13}$$

For the composite containing Ni nanoparticles (curve 1), the percolation threshold is observed near $V \approx 0.10$, which is significantly lower than that of the material with Ni microparticles, where the critical concentration is $V \approx 0.21$. The earlier formation of the infinite cluster in the nanostructured composite indicates a denser and more efficient particle-to-particle contact, as well as the emergence of extended, tunnel-connected chains that facilitate the development of a conductive network at a lower fraction of the conducting phase. The saturation of conductivity at high filler concentrations

($V \geq 0.3$) also differs: the nanocomposite exhibits a higher asymptotic value of σ, corresponding to an increase in the parameter σ_1 by more than an order of magnitude compared to the material containing micron-sized Ni particles. This reflects the formation of a more highly branched and structurally compact skeleton of the infinite cluster, which ensures efficient charge transport [38].

The inset in the graph ($dlg\sigma/dV_1$) illustrates differences in the width and amplitude of the derivative maxima, indicating a sharper and narrower percolation transition in the composite containing nanoparticles and, consequently, a more homogeneous distribution of conductive pathways. In the case of microparticles (curve 2), the transition is more extended, which reflects a higher degree of structural disorder and a smaller number of effective interparticle contacts.

Agreement between the experimental and theoretical values (Fig. 4) is observed for both types of composites at $V_1 > V_s$. For $V_1 < V_s$ such correspondence is maintained only for the composites containing micro-sized Ni particles. The origin of this discrepancy is discussed within the framework of the spatial–structural hierarchical model proposed in [39,40] for polymer-based composites. To determine the topology of the infinite cluster, the previously introduced percolation-theory expressions were employed. By applying the boundary condition at $V_1 = 1$, expressions (4), (8), and (10) can be rewritten in the form:

$$P(V_1) = D\left(\frac{V_1 - V_s}{1 - V_s}\right)^{\beta}, \tag{14}$$

$$\frac{Z}{R} = \left(\frac{V_1 - V_s}{1 - V_s}\right)^{(\nu - \xi)}, \tag{15}$$

$$\frac{P_{sk}(V_1)}{P(V_1)} = D\left(\frac{V_1 - V_s}{1 - V_s}\right)^{(2\nu - \beta)}, \tag{16}$$

The results indicate that the use of nanodispersed nickel leads to a significant reduction in the percolation threshold, a more intensive formation of the conducting network, and a substantial increase in the ultimate conductivity σ_1. This confirms the effectiveness of Ni nanoparticles as a highly efficient conductive filler for ceramic composites.

The values of $P(V_1)$ calculated from relation (14) approach unity as V_1 increases (see Tables 1 and 2), indicating the gradual densification of the infinite cluster due to the attachment of isolated clusters as the system moves away from the percolation threshold.

Table 1. Dependence of the parameters $P(V_1)$ $V_1^{/}$; Z/R; $V_1^{//}$ and $V_1^{///}$ on the filler volume fraction V_1 for composites containing nanodispersed Ni particles

no.	V_1	$P(V_1)$	$V_1^{/}$	Z/R	$V_1^{//}$	$V_1^{///}$
1	0.12	0.19	0.023	7.7	$2.1\cdot10^{-5}$	$2.29\cdot10^{-2}$
2	0.13	0.23	0.031	6.0	$6.5\cdot10^{-5}$	$3.09\cdot10^{-2}$
3	0.16	0.33	0.052	4.0	$4.1\cdot10^{-5}$	$5.19\cdot10^{-2}$
4	0.20	0.41	0.082	3.1	$1.8\cdot10^{-5}$	$8.19\cdot10^{-2}$
5	0.23	0.46	0.106	2.7	$3.7\cdot10^{-3}$	$1.02\cdot10^{-1}$
6	0.3	0.54	0.163	2.1	$1.2\cdot10^{-3}$	$1.6\cdot10^{-1}$
7	0.4	0.64	0.257	1.7	$3.2\cdot10^{-2}$	$2.2\cdot10^{-1}$
8	0.45	0.68	0.307	1.6	$6.0\cdot10^{-2}$	$2.4\cdot10^{-1}$
9	0.5	0.72	0.360	1.5	$8.9\cdot10^{-2}$	$2.7\cdot10^{-1}$

Table 2. Dependence of the parameters $P(V_1)$ $V_1^{/}$; Z/R; $V_1^{//}$ and $V_1^{///}$ on the filler volume fraction V_1 for composites containing microdispersed Ni particles

no.	V_1	$P(V_1)$	$V_1^{/}$	Z/R	$V_1^{//}$	$V_1^{///}$
1	0.22	0.17	0.037	1.42	$2.2\cdot10^{-4}$	$3.7\cdot10^{-2}$
2	0.25	0.30	0.075	1.27	$4.6\cdot10^{-4}$	$7.4\cdot10^{-2}$
3	0.30	0.42	0.125	1.19	$3.0\cdot10^{-3}$	$1.2\cdot10^{-1}$
4	0.35	0.50	0.175	1.15	$9.1\cdot10^{-3}$	$1.6\cdot10^{-1}$
5	0.40	0.57	0.224	1.12	$2.0\cdot10^{-2}$	$2.0\cdot10^{-1}$
6	0.45	0.62	0.279	1.10	$3.6\cdot10^{-2}$	$2.4\cdot10^{-1}$
7	0.5	0.66	0.334	1.08	$6.0\cdot10^{-2}$	$2.7\cdot10^{-1}$

The volume fraction of the infinite cluster V'_1, calculated using expression (3), represents only a small portion of V_1. in the vicinity of the percolation threshold. The values of Z/R, obtained from formula (15) in the threshold region, indicate a high tortuosity of the infinite cluster; the critical correlation-length exponent ν was taken as 0.85, whereas the tortuosity exponent ξ was determined from expression (5). Using formula (16) for $P_{sk}(V_1)$ and relation (7), the volume fractions of the backbone V_1'' and dangling ends $V_1''' = V_1'' - V_1'$ of the infinite cluster were evaluated. As follows from Tables 1 and 2, the volume fraction of the backbone near the percolation threshold constitutes only a small portion of the cluster, whereas the majority of nodes belong to the dangling ends.

Figure 5 shows the logarithmic dependence of the electrical conductivity for composite samples with Ni in the range $V_s < V_1 \leq V_a \approx 0.5$, containing Ni microparticles (curve 1) and nanoparticles (curve 2). The plot is constructed in the coordinates of relation (13), which makes it possible to identify the linear region corresponding to the percolation conduction regime.

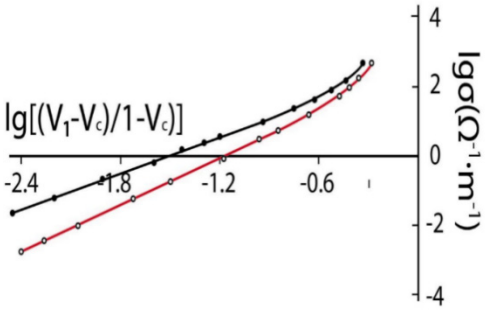

Figure 5. Logarithmic dependence of the electrical conductivity for composites with Ni microparticles (1) and nanoparticles (2).

The linear-growth regions are well approximated by the power-law dependence

$$\sigma = \sigma_1 (V_1 - V_s)^t, \tag{17}$$

which is characteristic of three-dimensional composites.

For both materials, a distinct percolation transition is observed: upon reaching the critical concentration V_s the electrical conductivity increases abruptly by several orders of magnitude. Linear extrapolation of the dependence to $V_1=1$ made it possible to determine the value of σ_1, which reflects the conductivity of a fully formed infinite cluster. For the composite filled with nickel nanoparticles, the obtained parameters are $V_s=0.105$, $t = 2.2$, and $\sigma_1 = 63\ \Omega^{-1}\cdot cm^{-1}$. In the case of the material containing micro-dispersed Ni particles, the critical concentration is $V_s=0.210$, the critical conductivity exponent is $t = 1.78$, and the conductivity of the formed cluster is $\sigma_1 = 8\ \Omega^{-1}\cdot cm^{-1}$

A comparative analysis of dependencies 1 and 2 shows that the introduction of nano-dispersed nickel results in an almost twofold reduction of the percolation threshold, as well as in an increase of the parameter σ_1 by more than an order of magnitude compared to the composite containing micro-sized Ni particles. This difference is attributed to the higher degree of interparticle contact among the nanoparticles and the formation of a quasi-continuous tunneling pathway for charge transport. The nanoscale filler forms a denser and more highly branched backbone of the infinite cluster, which leads to a significant increase in macroscopic conductivity [41–43]. It is important to note that σ_1 is not the conductivity of individual metallic particles; instead, it characterizes the effective conductivity of the percolation cluster in the range $V_s < V_1 \leq V_a \approx 0.5$, i.e., the conductivity of a branched fractal network through which the dominant charge transport occurs. The critical exponent q is taken as 1, which corresponds to three-dimensional percolation systems and agrees with literature data. Analysis of the logarithmic dependences demonstrates that nano-dispersed Ni is significantly more effective in forming a conductive network within the polymer matrix, ensuring higher composite conductivity at lower filler content [44-47].

CONCLUSIONS

The study of the topology of the infinite cluster in polymer composites containing micro- and nanosized Ni particles enabled quantitative determination of how particle size affects the parameters of the percolation transition and the configuration of the conductive network. It has been established that the use of nano-dispersed nickel leads to a significant reduction in the percolation threshold: for nanocomposites, the critical concentration is $V_c \approx 0.105$, whereas for materials with micro-dispersed Ni it reaches $V_s \approx 0.21$. This reflects more efficient interparticle contact among nanoparticles and earlier formation of the infinite cluster.

The introduction of Ni nanoparticles enhances the efficiency of conductive network formation, providing an almost twofold reduction of the percolation threshold, an increase of the parameter σ_1 by more than an order of magnitude, a sharper and more localized percolation transition, and the development of an extended, coherent conductive structure at a lower volume fraction of the metallic phase. The obtained dependences $P(V_1)$, $\xi(V_1)$ and $P_{sk}(V_1)$ demonstrate gradual densification of the cluster with increasing concentration of the conducting phase, with rapid saturation of connections at $V_1 \approx 0.4$-0.5. The topological parameters (correlation radius R, tortuosity exponent ξ, and the volume fractions V_{1sk} and V_{1mk}) are consistent with classical fractal percolation theory, and the adopted critical exponent $\nu = 0.85$ provides an accurate description of cluster behavior near the threshold. At identical values of V_1 the density of the infinite cluster in nanostructured systems is significantly higher, which accelerates the formation of a conductive network.

The structure of the infinite cluster exhibits pronounced fractal–hierarchical characteristics. The fractal dimension of the skeletal part ranges from 1.6 to 1.8, whereas for the dead ends it ranges from 1.9 to 2.1, reflecting substantial structural heterogeneity near the percolation threshold. The volume fraction of the dead ends significantly exceeds that of the skeletal bonds: for example, at

V_1= 0.12 the skeletal fraction in the nanocomposite is only 0.023, while the fraction of dead ends exceeds $2 \cdot 10^{-5}$; for the microcomposite at V_1=0.22 the skeletal fraction is merely 0.037. Such a ratio $V_{1sk} \ll V_{1mk}$ limits the transport efficiency of the system in the immediate vicinity of the threshold.

The density of the infinite cluster, the correlation radius, and other topological parameters follow power-law scaling characteristic of three-dimensional percolation. The critical conductivity exponents are 2.2 for nano-dispersed Ni and 1.78 for micro-dispersed Ni, which agree with universal values and confirm the influence of branch tortuosity on the increase of *t*. At high filler concentrations ($V \geq 0.3$), nanostructuring leads to a substantial rise in the asymptotic conductivity. The conductivity parameter of the skeleton reaches 63 $\Omega^{-1} \cdot cm^{-1}$, for the nanocomposite and 8 $\Omega^{-1} \cdot cm^{-1}$ for the composite containing micro-sized Ni particles, corresponding to an increase by a factor of more than 7–8. This enhancement is attributed to the formation, in nanocomposites, of a denser, more highly branched, and topologically saturated structure of the infinite cluster.

The analysis indicates that incorporating Ni nanoparticles substantially enhances the efficiency of conductive network formation in the composites. Their use leads to an almost twofold reduction in the percolation threshold, an order-of-magnitude increase in the parameter σ_1, and the emergence of a sharper and more localized percolation transition. In addition, Ni nanoparticles promote the development of a more extended and interconnected conductive network at significantly lower metal filler contents. The results demonstrate the high effectiveness of Ni nanoparticles as a conductive filler and provide a solid scientific basis for designing next-generation high-conductivity composites.

ORCID

Zafarjon M. Khusanov, https://orcid.org/0009-0005-9420-8033; **Fakhriddin T. Boymuratov,** https://orcid.org/0000-0003-1703-4605; **Sardor G'. To'ychiyev,** https://orcid.org/0009-0008-3522-5791

REFERENCES

[1] Ye.P. Mamunya, V. Davydenko, P. Pissis, and E.V. Lebedev, "Electrical and thermal conductivity of polymers filled with metal powders," European Polymer Journal, **38**(9), 1887-1897 (2002). https://doi.org/10.1016/S0014-3057(02)00064-2

[2] R. Zakirov, and F. Giyasova, "Application of Fiber-Optic Sensors for the Aircraft Structure Monitoring," in: *Safety in Aviation and Space Technologies. Lecture Notes in Mechanical Engineering*, edited by A. Bieliatynskyi, and V. Breskich, (Springer, Cham., 2022). https://doi.org/10.1007/978-3-030-85057-93

[3] Sh.I. Klychev, S.A. Bakhramov, O.R. Parpiev, M.S. Paizullakhanov, L.S. Suvonova, D.E. Kadyrgulov, E.K. Matjanov, & F.A. Giyasova, "Optical-Energy Characteristics and Heating Temperatures in Small Single-Mirror Solar Furnaces," Applied Solar Energy, **60**(5), 703-707 (2025). https://doi.org/10.3103/S0003701X24602394

[4] A. Prokopchuk, I. Zozulia, Yu. Didenko, and D. Tatarchuk, "Henning Heuer and Yuriy Poplavko. Dielectric Permittivity Model for Polymer–Filler Composite Materials by the Example of Ni- and Graphite-Filled Composites for High-Frequency Absorbing Coatings," Coatings, **11**(2), 172 (2021). https://doi.org/10.3390/coatings11020172

[5] N. Sarikhani, Z.S. Arabshahi, A.A. Saberi, and A.Z. Moshfegh, "Unified modeling and experimental realization of electrical and thermal percolation in polymer composites," Appl. Phys. Rev. **9**, 041403 (2022). https://doi.org/10.1063/5.0089445

[6] M. Majidian, C. Grimaldi, L. Forró, & A. Magrez, "Role of the particle size polydispersity in the electrical conductivity of carbon nanotube-epoxy composites," Scientific Reports, **7**, 12553 (2017). https://doi.org/10.1038/s41598-017-12857-8

[7] J. Payandehpeyman, and M. Mazaheri, "Geometrical and physical effects of nanofillers on percolation and electrical conductivity of polymer carbon-based nanocomposites: a general micro-mechanical model," Soft Matter, **19**, 530-539 (2023). https://doi.org/10.1039/D2SM01168A

[8] M.-Á.M. Cruz, J.P. Ortiz, M.P. Ortiz, and A. Balankin, "Percolation on Fractal Networks: A Survey," Fractal Fract. **7**(3), 231 (2023). https://doi.org/10.3390/fractalfract7030231

[9] X. Nan, Y. Zhang, J. Shen, R. Liang, J. Wang, L. Jia, X. Yang, *et al*., "A Review of the Establishment of Effective Conductive Pathways of Conductive Polymer Composites and Advances in Electromagnetic Shielding," Polymers, **16**(17), 2539 (2024). https://doi.org/10.3390/polym16172539

[10] X. Chao, W. Tian, F. Xu, & D. Shou, "A fractal model of effective mechanical properties of porous composites," Composites Science and Technology, **213**, Article 108957 (2021). https://doi.org/10.1016/j.compscitech.2021.108957

[11] R.M. Mutiso, and K.I. Wineyn, "7.17 - Electrical Conductivity of Polymer Nanocomposites," Polymer Science: A Comprehensive Reference, **7**, 327-344 (2012). https://doi.org/10.1016/B978-0-444-53349-4.00196-5

[12] F. Pargi, P.L. Teh, S. Husseinsyah, and C.K. Yeoh, "Recycled-copper-filled epoxy composites: the effect of mixed particle size," International Journal of Mechanical and Materials Engineering, **10**(1), (2015). https://doi.org/10.1186/s40712-015-0030-2

[13] I.Y. Forero-Sandoval, A.P. Franco-Bacca, F. Cervantes-Álvarez, C.L. Gómez-Heredia, J.A. Ramírez-Rincón, J. Ordonez-Miranda, and J.J. Alvarado-Gil, "Electrical and thermal percolation in two-phase materials: A perspective," J. Appl. Phys. **0131**, 230901 (2022). https://doi.org/10.1063/5.0091291

[14] L. Zhang, W. Wang, X. Wang, P. Bass, and Z.-Y. Cheng, "Metal-polymer nanocomposites with high percolation threshold and high dielectric constant," Appl. Phys. Lett. **103**, 232903 (2013). https://doi.org/10.1063/1.4838237

[15] T. Kasagi, K. Goda, & S. Yamamoto, "Complex Permittivity Spectra of Granular Polymer Composites with Dispersed Ag-Coated Cu Flakes," J. Electron. Mater, **53**, 7865-7875 (2024). https://doi.org/10.1007/s11664-024-11450-w

[16] J. Agrisuelas, R. Balart, J.J. García-Jareño, J. López-Martínez, and F. Vicente, "A Macroscopic Interpretation of the Correlation between Electrical Percolation and Mechanical Properties of Poly - (Ethylene Vinyl Acetate)/Zn Composites," Materials, **17**(11), 2527 (2024). https://doi.org/10.3390/ma17112527

[17] Y. Wang, H.A. Moghaddam, J.P. Moreno, and P. Mertiny, "Magnetic Filler Polymer Composites-Morphology Characterization and Experimental and Stochastic Finite Element Analyses of Mechanical Properties," Polymers, **15**(13), 2897 (2023). https://doi.org/10.3390/polym15132897

[18] G.V. Martyniuk, and O.I. Aksimentyeva, "Percolation phenomena in the polymer composites with conducting polymer fillers," Physics and Chemistry of Solid State, **22**(4), 811-816 (2021). https://doi.org/10.15330/pcss.22.4.811-816
[19] S.-U. Kim, and J.-Y. Kim, "Dynamic Statistical Mechanics Modeling of Percolation Networks in Conductive Polymer Composites for Smart Sensor Applications," Materials, **18**(13), 3097 (2025). https://doi.org/10.3390/ma18133097
[20] Z. Zhang, L. Hu, R. Wang, S. Zhang, L. Fu, M. Li, and Q. Xiao, "Advances in Monte Carlo Method for Simulating the Electrical Percolation Behavior of Conductive Polymer Composites with a Carbon-Based Filling," Polymers, **16**(4), 545 (2024). https://doi.org/10.3390/polym16040545
[21] F.R. Beltrán, H. Aksas, L.S. Salah, Y. Danlée, and I. Huynen, "Theoretical Prediction of Electrical Conductivity Percolation of Poly (lactic acid)-Carbon Nanotube Composites in DC and RF Regime," Materials, **16**(15), 5356 (2023). https://doi.org/10.3390/ma16155356
[22] Y. Huang, C. Ellingford, C. Bowen, T. McNally, D. Wu, & C. Wan, "Tailoring the electrical and thermal conductivity of multi-component and multi-phase polymer composites," International Materials Reviews, **65**(3), 129-163 (2020). https://doi.org/10.1080/09506608.2019.1582180
[23] H. Liu, X. Ji, W. Wang, and L. Zhou, "3D-Networks Based Polymer Composites for Multifunctional Thermal Management and Electromagnetic Protection: A Mini Review," Materials, **17**(10), 2400 (2024). https://doi.org/10.3390/ma17102400
[24] A.A. Reffaee, A.A. Ward, & A.I. Khalaf, "Structural, magnetic and dielectric properties of waste magnetic filler rubber nanocomposites,' Polym. Bull. **81**, 3081-3105 (2024). https://doi.org/10.1007/s00289-023-04835-0
[25] A. Gunya, J. Kúdelčík, Š. Hardoň, and M. Janek, "Thermodielectric Properties of Polyurethane Composites with Aluminium Nitride and Wurtzite Boron Nitride Microfillers: Analysis Below and near Percolation Threshold," Sensors, **25**(13), 4055 (2025). https://doi.org/10.3390/s25134055
[26] O.I. Vernaya, V.V. Epishev, M.A. Markov, V.A. Nuzhdina, V.V. Fedorov, V.P. Shabatin, T.I. Shabatina, "Synthesis of Copper Nanoparticles by Thermal Decomposition of Anhydrous Copper Formate," Moscow Univ. Chem. Bull. **72**, 267–268 (2017). https://doi.org/10.3103/S0027131417060074
[27] G. Yurkov, A. Kozinkin, S. Kubrin, A. Zhukov, S. Podsukhina, V. Vlasenko, A. Fionov,et *al*., "Nanocomposites Based on Polyethylene and Nickel Ferrite: Preparation, Characterization, and Properties," Polymers, **15**(19), 3988 (2023). https://doi.org/10.3390/polym15193988
[28] S.V. Roth, R. Döhrmann, M. Dommach, M. Kuhlmann, I. Kröger, R. Gehrke, H. Walter, *et al*., Small-angle options of the upgraded ultrasmall-angle x-ray scattering beamline BW4 at HASYLAB," Rev. Sci. Instrum. **77**, 085106 (2006). https://doi.org/10.1063/1.2336195
[29] A. Umarov, U. Abdurakhmanov, Ya. Raximova, M. Karaboeva, D. Saidqulov, and F. Boymuratov, "Study of the electro and thermophysical properties of composite ceramic materials containing nickel nanoparticles," E3S Web of Conferences (*XXVI International Scientific Conference "Construction the Formation of Living Environment" (FORM-2023)*, **410**, 02060 (2023). https://doi.org/10.1051/e3sconf/202341002060
[30] G. Psarras, "Conductivity and dielectric characterization of polymer nanocomposites," in: *Physical Properties and Applications of Polymer Nanocomposites*, (2010), pp.31-69. https://doi.org/10.1533/9780857090249.1.31
[31] A.S. Skal, & B.I. Shklovskii, "Topology of an infinite cluster in the theory of percolation and its relationship to the theory of hopping conduction," Sov. Phys. Semicond. **8**(8), 1029-1032 (1975).
[32] R. Ma, G. Mu, H. Zhang, and J. Liu, "Percolation analysis of the electrically conductive network in a polymer nanocomposite by nanorod functionalization," RSC Advances, **9**(62), 36324-36333 (2019). https://doi.org/10.1039/C9RA04680A
[33] G. Paul, S.V. Buldyrev, N.V. Dokholyan, S. Havlin, P.R. King, Y. Lee, and H.E. Stanley, "Dependence of Conductance on Percolation Backbone Mass," Phys. Rev. E, **61**, 3435 (2000). https://doi.org/10.1103/PhysRevE.61.3435
[34] A. Herega, "Some Applications of the Percolation Theory: Review of the Century Beginning," Journal of Materials Science and Engineering A, **5**(11-12), 409-414 (2015). https://doi.org/10.17265/2161-6213/2015.11-12.004
[35] A.G. Hunt, and M. Sahimi, "Flow, Transport, and Reaction in Porous Media: Percolation Scaling, Critical-Path Analysis, and Effective Medium Approximation," Reviews of Geophysics, **55**(4), 993-1078 (2017). https://doi.org/10.1002/2017RG000558
[36] Kh.S. Daliev, and Z.M. Khusanov, "Properties of Single Crystal Silicon Doped with Vanadium," East European Journal of Physics, (1), 366-369 (2024). https://doi.org/10.26565/2312-4334-2024-1-35
[37] T.M. Razikov, S.A. Muzafarova, R.T. Yuldoshov, Z.M. Khusanov, M.K. Khusanova, Z.S. Kenzhaeva, and B.V. Ibragimov, **"**Growing Sb_2Se_3 films enriched with selenium using chemical molecular beam deposition," East European Journal of Physics, (1), 370-374 (2024). https://doi.org/10.26565/2312-4334-2024-1-36
[38] Z.T. Azamatov, V.E. Gaponov, A.A. Jeenbekov, and A.B. Bakhromov, "Digital Shearograph for Detecting Defect in Materials," Russian Microelectronics, **52**, Suppl 1, S263 (2023). https://doi.org/10.1134/S106373972360019X
[39] W. Bauhofer, and J.Z. Kovacs, "A review and analysis of electrical percolation in carbon nanotube polymer composites," Composites Science and Technology, **69**(10), 1486-1498 (2009). https://doi.org/10.1016/j.compscitech.2008.06.018
[40] O. Folorunso, Y. Hamam, R. Sadiku, S.S. Ray, and A.G. Joseph, "Parametric Analysis of Electrical Conductivity of Polymer-Composites," Polymers, **11**(8), 1250 (2019). https://doi.org/10.3390/polym11081250
[41] I. Balberg, D. Azulay, D. Toker, and O. Millo, "Percolation and Tunneling in Composite Materials," International Journal of Modern Physics B, **18**(15), (2004). https://doi.org/10.1142/S0217979204025336
[42] U. Abdurakhmanov, A.V. Umarov, M.I. Raximova, amd M. Karabayeva, "An Investigation of the Electrophysical Properties of Composite Ceramic Materials Containing Nickel Nanoparticles," Research Letters in Physical Chemistry, **8**, 231-239 (2023). https://doi.org/10.22036/pcr.2022.335151.2063
[43] H. Pang, L. Xu, D.-X. Yan, and G. Zhong, "Conductive Polymer Composites with Segregated Structures," Progress in Polymer Science, **39**(11), (2014). https://doi.org/10.1016/j.progpolymsci.2014.07.007
[44] A.V. Karimov, D.M. Yodgorova, F.A. Giyasova, E.M. Shpilevskiy, & N.I. Usmanova, "Photovoltatic Effect in Au-nSi-Au Structures with Schottky Barriers and Features of Spectral Characteristics, Applied Solar Energy, **54**, 330-332 (2018). https://doi.org/10.3103/S0003701X18050109

[45] K.A. Ismailov, Z.M. Saparniyazova, G.T. Kudeshova, G.A. Seytimbetova, and F.A. Saparov, "Influence of doping conditions on the properties of Nickel atomic clusters," East Eur. J. Phys. (1), 327 (2024). https://doi.org/10.26565/2312-4334-2024-1-30
[46] S.I. Vlasov, F.A. Saparov, and K.A. Ismailov, "Effect of pressure on the characteristics of Schottky barrier diodes made of overcompensated semiconductor," Semiconductor physics, quantum electronics & optoelectronics, **13**(4), 363-365 (2010). http://journal-spqeo.org.ua/n4_2010/v13n4-2010-p363-365.pdf
[47] A.Yu. Leyderman, R.A. Ayukhanov, R.M. Turmanova, A.K. Uteniyazov, and E.S. Esenbaeva, "Non-recombination injection mode," Semiconductor Physics, Quantum Electronics and Optoelectronics, 24(3), 248-254 (2021). https://doi.org/10.15407/spqeo24.03.248

ТОПОЛОГІЧНІ ОСОБЛИВОСТІ ФОРМУВАННЯ ПРОВІДНОЇ МЕРЕЖІ В МЕТАЛОПОЛІМЕРНИХ КОМПОЗИТАХ З РІЗНИМИ РОЗМІРАМИ ЧАСТИНОК НАПОВНЮВАЧА

Зафарджон М. Хусанов[1], Фахріддін Т. Боймуратов[2], Сардор Г. Тойчієв[1]
[1]Кіберуніверситет, Нурафшан, Узбекистан
[2]Університет Альфраганус, Ташкент, Узбекистан

Було досліджено топологію нескінченного кластера в полімерних композитах, що містять мікро- та наночастинки Ni, що дозволило кількісно оцінити, як розмір провідних частинок впливає на перколяційний перехід та структуру провідної мережі. Використання нанорозмірного Ni знижує критичну концентрацію до Vs ≈ 0,105 порівняно з Vs ≈ 0,21 для мікрочастинок, збільшує параметр σ_1 більш ніж на порядок та призводить до різкішого, більш локалізованого перколяційного переходу. Кластерна структура демонструє виражені фрактально-ієрархічні особливості: фрактальна розмірність остова становить 1,6-1,8, а звисаючих кінців – 1,9-2,1. Щільність кластерів, радіус кореляції та топологічні параметри відповідають степеневим співвідношенням, типовим для тривимірної перколяції (ν = 0,85). При високих концентраціях провідної фази (V ≥ 0,3) асимптотична провідність досягає 63 $\Omega^{-1}\cdot см^{-1}$ у нанокомпозитах порівняно з 8 $\Omega^{-1}\cdot см^{-1}$ для матеріалів на основі мікрочастинок. Ці результати підтверджують високу ефективність наночастинок нікелю у формуванні протяжної, взаємопов'язаної та розгалуженої провідної мережі, що забезпечує основу для високопровідних композитів наступного покоління.

Ключові слова: *полімерні композити; наночастинки нікелю; мікрочастинки; нескінченний кластер; провідна мережа; асимптотична провідність; топологічні параметри; тривимірна перколяція*